Interconnect Fabrication by Superconformal Iodine-Catalyzed Chemical Vapor Deposition of Copper

D. Josell,[a,z] Sibum Kim,[b] D. Wheeler,[a] T. P. Moffat,[a,*] and Sung Gyu Pyo[b]

[a]*Metallurgy Division, National Institute of Standards and Technology, Gaithersburg, Maryland, USA*
[b]*Hynix Semiconductor Incorporated, Korea*

The mechanism behind superconformal filling of fine features during surfactant catalyzed chemical vapor deposition (CVD) is described and the metrology required to predict it is identified and quantified. The impact of adsorbed iodine coverage on copper deposition rate during chemical vapor deposition of copper on planar substrates is determined first. These kinetic parameters are then used in a model based on the curvature-enhanced accelerator coverage mechanism to predict superconformal filling during iodine-catalyzed CVD. In this model, the coverage of the adsorbed catalyst is presumed to change with surface area during interface evolution. The surface area decreases along the bottoms of submicrometer dimension features, increasing the local coverage and deposition rates and thereby enabling superconformal filling. Experimental filling results are then described and shown to be consistent with the predictions.
© 2003 The Electrochemical Society. [DOI: 10.1149/1.1566960] All rights reserved.

Recent publications have described the curvature-enhanced accelerator coverage (CEAC) mechanism[1,2] and successfully used it to predict superconformal filling of fine features during copper and silver electrodeposition in trenches and vias.[1-6] Quantitative predictions were made for filling over a wide range of experimental conditions and feature dimensions using kinetic parameters obtained solely from studies on planar substrates.[1-5] The CEAC mechanism involves (1) the adsorption of a catalyst that enhances metal deposition rates and (2) local increase (decrease) of the catalyst coverage with decrease (increase) of local surface area during growth on rough or patterned surfaces. This mechanism leads directly to superconformal film growth within submicrometer dimension trenches and vias. The predictions of CEAC-based models accurately describe all aspects of superconformal filling electrodeposition experiments, including an initial "incubation period" of conformal growth, whether bottom-to-top "superfill" itself occurs or does not occur, and the ultimate development of an overfill bump, a manifestation of so-called "momentum" plating.

Superconformal filling during iodine-catalyzed chemical vapor deposition (CVD) in vias has recently been described.[7-12] Unlike papers published during the early years of superconformal electrodeposition, it has been generally recognized that the likely mechanism is the local increase of coverage of adsorbed iodine catalyst at the bottoms of the fine features due to area decrease during growth.[c,8-11] Indeed, predictions of superconformal filling during surfactant catalyzed CVD have already been made by one group[10] using a CEAC-based model and independently obtained kinetics.[12] Quantitative comparisons of predictions to experiments were not made. This work makes such comparisons.

Experimental

Specimen preparation.—Specimens were prepared from either planar or lithographically patterned substrates. Unless otherwise indicated, patterned features included a TiN barrier ~30 nm thick and a copper seed ~25 nm thick, both deposited by conventional CVD. For catalyzed CVD, iodine was adsorbed on the specimen surface by bubbling carrier gas through the iodine precursor CH_2I_2 held at 80°C then over the substrates, held at 150°C in the reactor, for a specified amount of time. The iodine coverage thus obtained was determined from total reflection X-ray flourescence (TXRF) studies with unpatterned specimens. Figure 1 shows the measured depen-

dence of the iodine coverage on the exposure time. Both the iodine adsorption and the copper metal deposits were made in a 200 mm Apex model Cruise-200M reactor.[d] The copper was deposited using Cu(I)-hexafluoroacetylacetonate-vinyltrimethylsilane, [(hfac)Cu-(vtms)], precursor (Cupra SelectTM2504)[d] that was vaporized and introduced to the reactor using a Bronhorst[d] liquid source delivery system with H_2 as the carrier gas. The precursor consumption rate was 0.5 cm³/min.

Deposition on planar substrates.—The impact of the adsorbed iodine on the copper deposition rate was determined from studies of metal deposition on planar substrates. Deposition rates were determined from the deposit thickness, obtained by cross-sectional scanning electron microscopy (SEM) and/or transmission electron microscopy (TEM) and the deposition time. The dependence of the metal deposition rate on the iodine exposure time is shown in Fig. 2a as a function of exposure time (*i.e.*, coverage). The same data is shown in Fig. 2b as a function of reciprocal temperature; data from Ref. 12 for no iodine coverage and 0.1 monolayers (*i.e.*, copper site coverage) of iodine are overlaid. The different deposition rates observed in the two studies when there is no iodine, a factor of two for the data at both 150 and 170°C, are necessarily associated with differences in the delivery of copper precursor to the specimens; differences due to nucleation on the different substrate materials are not believed to be significant. The data is therefore replotted in Fig. 2c with all deposition rates from Ref. 12 divided by a factor of two to minimize differences due to the ambient concentration of copper precursor in order to permit comparison of the impact of iodine coverage alone. Based on the changing slope, control of the metal deposition rate is shifting from the iodine-determined interface kinetics at the lower temperatures and iodine coverages to deposition controlled by transport of the (hfac)Cu(vtms) precursor at the higher temperatures and iodine coverages. This occurs at a similar scaled deposition rate on the surface with the 0.1 monolayer coverage of iodine (Fig. 2c). The data at 150°C, for which the deposition rate is not transport limited, is plotted in Fig. 3 as a function of the iodine coverage. A data point for surface coverage of 0.1 monolayers is also shown. This value is an extrapolation to 150°C of the scaled data between 50 and 100°C (Fig. 2c) for which the deposition rate was not transport limited. In light of the "estimated" coverage, the extrapolation over temperature, the use of continuous iodine doping using C_2H_5I in Ref. 12 as opposed to iodine adsorption from CH_2I_2 prior to metal deposition used here, and the scaling to account for different copper precursor delivery systems, the dependences of deposition rate on iodine coverage (Fig. 3) are in good agreement.
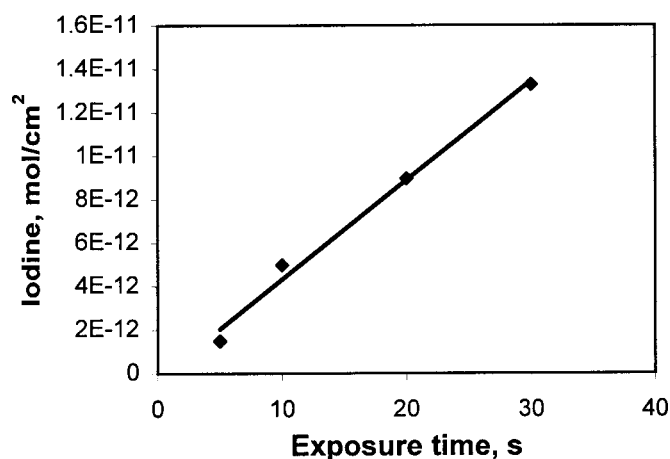
Figure 1. The dependence of the iodine coverage obtained as a function of time that the planar substrates were exposed to the CH_2I_2 precursor vapor (bubbling temperature 80°C) with substrate temperature 150°C. The linear fit to the data is indicated.

Comparison of the transport limited-deposition rate data at the highest temperature with the data of Ref. 12 provides no additional insight because the deposition kinetics in this regime are system dependent.

For the remainder of this work, adsorbed iodine coverages are expressed in terms of the fraction θ of the estimated saturation coverage 2.9×10^{-10} mol/cm^2,[13-15] which equals one-third of the total copper sites on a (111) copper surface.

Deposition on patterned substrates.—Figure 4 shows the superconformal filling of vias 1 μm high and aspect ratio 4 (height/diameter) at 120°C. The catalyst adsorbed inside the via has induced filling to occur in the bottom-to-top mode characteristic of superconformal filling. Figure 5 shows different aspects of the superconformal filling of 1 μm deep and aspect ratio 1.3 (height/width) trenches at 150°C: the initially conformal deposition (at 50 s), the inception of superconformal filling at the bottom corners (at 150 s) and the overfill bump (at 420 s). An increase from 150 to 170°C, coupled with an increase in aspect ratio from 3 to 3.5, results in a shift from superconformal (Fig. 6a) to subconformal (Fig. 6b) filling of trenches. Variability in fill times is evident from the specimen filled at 150°C (Fig. 6a, the overfill bump at the far left and the three-quarter filled trench in the middle). The thicker deposits toward the top of the specimen filled at 170°C (Fig. 6b) are consistent with copper precursor depletion down the trench arising from transport-limited deposition (as per Fig. 2c). In all cases, based on the 30 s iodine adsorption prior to the metal deposition, the initial iodine surface coverage is $\theta_o = 0.05$. A "soft" plasma treatment was used to remove iodine adsorbed over the features;[16] the impact on iodine coverage within the features, though believed to be minimal, has not been quantified.

Modeling Feature Filling

The model.—Modeling of interface evolution is done using a recently published CEAC-based formalism.[10] The dependence of metal deposition rate, *i.e.*, velocity, v, on local coverage of adsorbed iodine, θ, is expressed as

$$v(\theta,T) = (1 - \theta)v(0,T) + \theta v(1,T) \qquad [1]$$

for θ:[0,1] with the temperature dependent deposition rates on uncatalyzed and fully catalyzed surfaces $v(0,T)$ and $v(1,T)$, respectively. Generally, the dependence of the deposition rate on the coverage of catalyst need not be linear. As per the results obtained from Fig. 3 and the definition of the maximum iodine coverage, the relationship
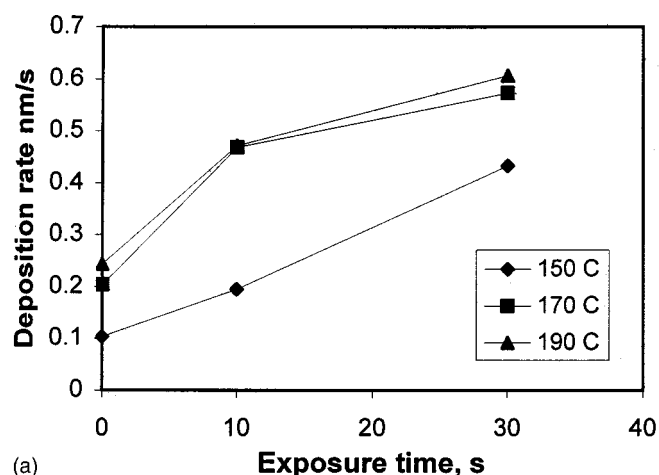
(a)
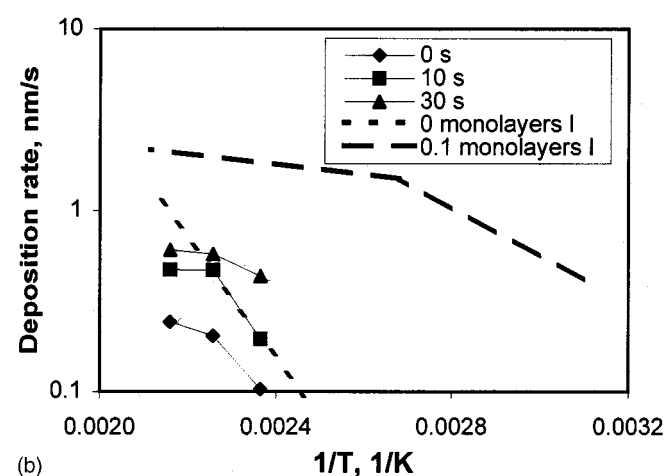
(b)
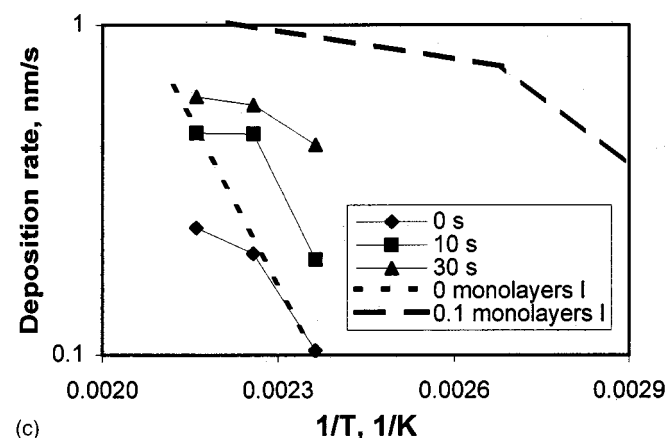
(c)

Figure 2. (a) The dependence of the copper deposition rate on the iodine exposure time is shown for different metal deposition temperatures. (b) The same data is replotted *vs.* reciprocal temperature. Data from Ref. 12 (dashed lines) has been overlaid. Different copper precursor delivery conditions are the likely source of the different behaviors. (c) Data replotted with the deposition rates from Ref. 12 were scaled by 0.5 to bring iodine-free results into agreement and thus account for copper precursor differences. Deposition rates in b and c are plotted on a log scale. Lines between data points are intended only to guide the eye.

$$v(\theta, \ 150°C) \approx 0.1 + 7\theta \ \text{nm/s} \qquad [2]$$

is used for modeling at 150°C. The deposition rate is presumed to stop increasing once θ reaches unity coverage. The expression
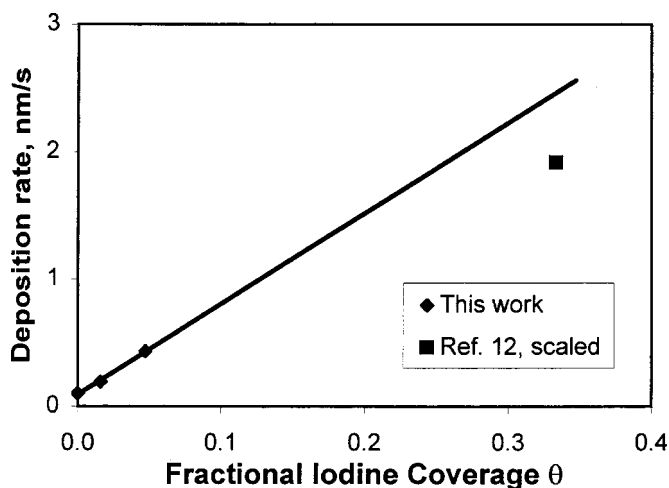
Figure 3. The dependence of the copper deposition rate on the iodine coverage. The data is consistent with a linear dependence (best fit is indicated). A value based on data from Ref. 12 is also included.

$$v_1(\theta,T) = (1 - \theta)1.55 \times 10^7 \exp\left(- \frac{7698}{T}\right) + \theta 5.6$$

$$\times 10^3 \exp\left(- \frac{3007}{T}\right) \text{ nm/s} \qquad [3]$$

with T in Kelvin, was previously used[10] for temperatures between 100 and 300°C. Based on Eq. 3, the maximum increase of metal deposition rate associated with catalyst coverage, *i.e.*, $v_1(1,T)/v_1(0,T)$, decreases from ≈ 90 down to only 1 as the temperature increases from 100 and 300°C. Generally, the higher this ratio, the higher the aspect ratio of features that can be filled.

For comparison, Eq. 3 yields $v_1(1, 150°C)/v_1(0, 150°C) = 24$ while Eq. 2 yields $v(1, 150°C)/v(0, 150°C) = 75$. The lower value
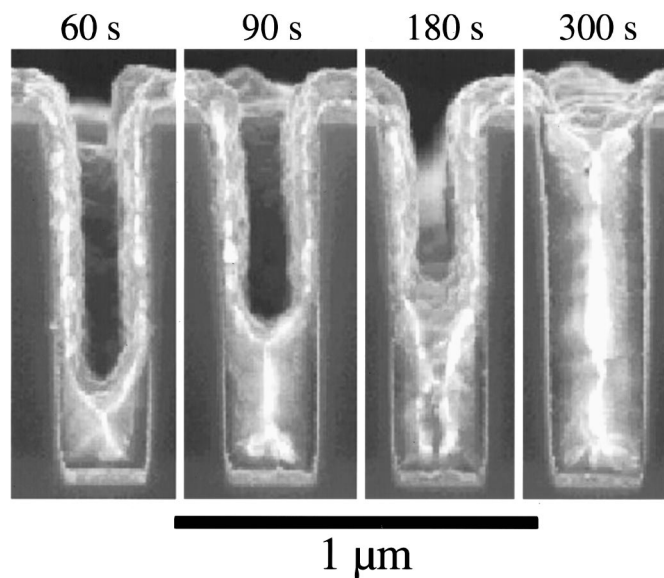
Figure 4. Vias of 1 μm height and 0.25 μm width after indicated deposition times. Bottom-to-top filling characteristic of the superconformal filling process is evident. Deposition temperature 120°C and initial iodine coverage of 1.3×10^{-11} mol/cm^2 (corresponding to $\theta_o \approx 0.05$) is based on a 30 s exposure to CH_2I_2 precursor vapor as per Fig. 1. The barrier layer and copper seed layer are 30 and 25 nm thick, respectively.
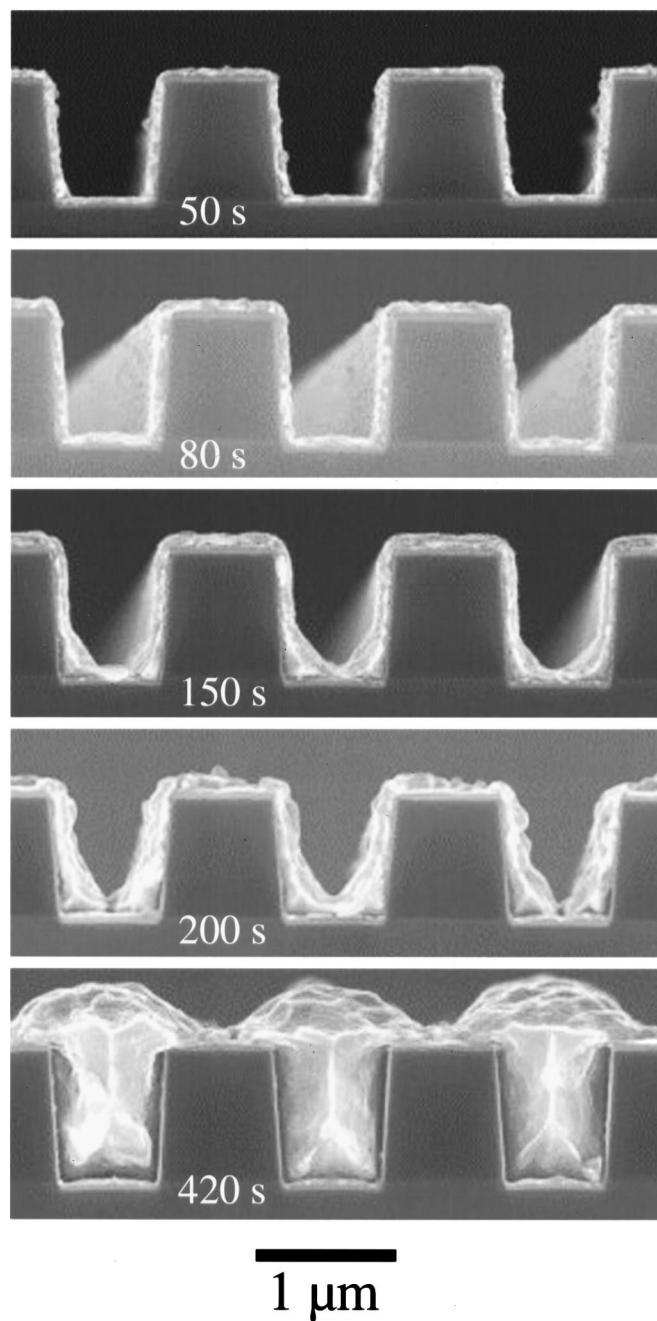
Figure 5. Trenches of 1 μm height and 0.6 μm width after different metal deposition times: conformal deposition at 50 s, inception of superconformal filling at the bottom corners at 150 s, formation of the overfill bump after 420 s. Deposition temperature 150°C and initial iodine coverage of 1.3 $\times 10^{-11}$ mol/cm^2 (corresponding to $\theta_o \approx 0.05$) is based on a 30 s exposure to CH_2I_2 precursor vapor as per Fig. 1. The barrier layer and copper seed layer are 30 and 25 nm thick, respectively.

for Eq. 3 reflects how the deposition rate data of Ref. 12 for 0.1 monolayers iodine coverage (Fig. 2b) was interpreted. In Ref. 10, this data was presumed to reflect the deposition rates for an iodine saturated surface (*i.e.*, for $\theta = 1$); if a value of $\theta = 0.33$ had been used, consistent with the one-third monolayer definition used here for the maximum coverage, the resulting form for $v_1(\theta,T)$ would have yielded $v_1(1, 150°C)/v_1(0, 150°C) = 72$, in agreement with the result obtained here.

Consistent with the agreement of temperature dependence evident in Fig. 2c, the kinetics obtained at 150°C are extrapolated to
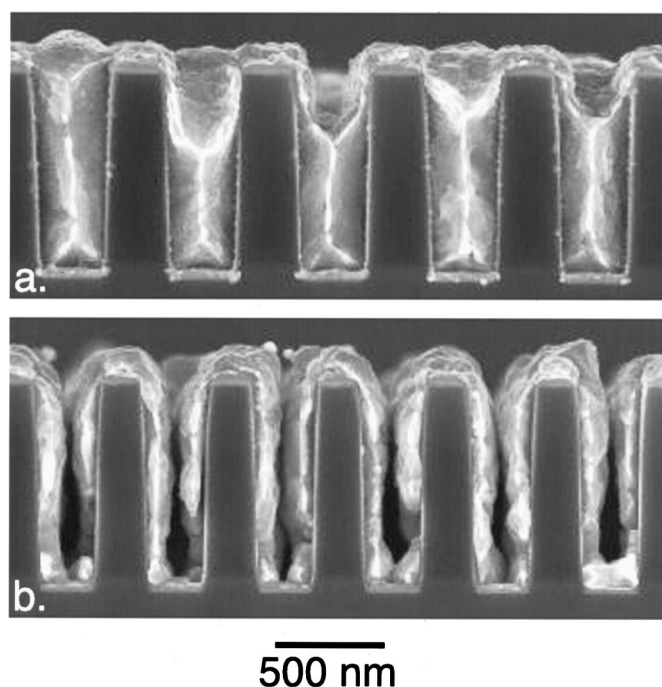
Figure 6. Experimental dependence of trench filling on the temperature. (a) Filling is superconformal for trenches with aspect ratio 3 filled at 150°C. (b) Filling is conformal for trenches with aspect ratio 3.5 at 170°C. The trenches are 1 μm deep. In both cases, iodine coverage is 1.3×10^{-11} mol/cm^2 (corresponding to $\theta_o \approx 0.05$) based on a 30 s exposure to CH$_2$I$_2$ precursor vapor as per Fig. 1.

other temperatures using a temperature dependence similar to that in Eq. 3, *i.e.*

$$v(\theta,T) = 0.1\exp\left[- 7698\left(\frac{1}{T} - \frac{1}{423}\right)\right]$$

$$+ \theta 7 \exp\left[- 3007\left(\frac{1}{T} - \frac{1}{423}\right)\right] \text{ nm/s} \quad [4]$$

Note that Eq. 4 reduces to Eq. 2 at 150°C.

Conservation of the adsorbed iodine catalyst for the case where there is no time-dependent accumulation, is summarized in Eq. 5

$$\frac{d\theta}{dt} = \kappa v \theta \quad [5]$$

which accounts for coverage change caused by the changing area, the rate of local area change being equal to the local curvature κ times the normal velocity v. While a term that characterizes the effect of consumption can be added, such consumption is reported to be negligible for iodine-catalyzed copper CVD.[8,12]

The kinetics and conservation rules given in Eq. 4 and 5, respectively, were implemented using a string model to track the moving interface and the local catalyst coverage;[1] filling of vias was modeled using a code that accounted for the sum of both curvature components in the cylindrical geometry. As noted earlier, transport limit-induced depletion of the metal precursor above and within the features was ignored in the simulations. Only the interface kinetics and the impact of iodine on local deposition rates through the CEAC mechanism are modeled. Failure to fill superconformally in the predictions is therefore indicated by formation of a seam, characteristic of conformal growth,[1] rather than a void within the feature.[2] Earlier simulations indicated that filling should vary substantially with the initial catalyst coverage, θ_o, and deposition temperature.[10] Those simulations predicted that lower θ_o and/or lower deposition tem-
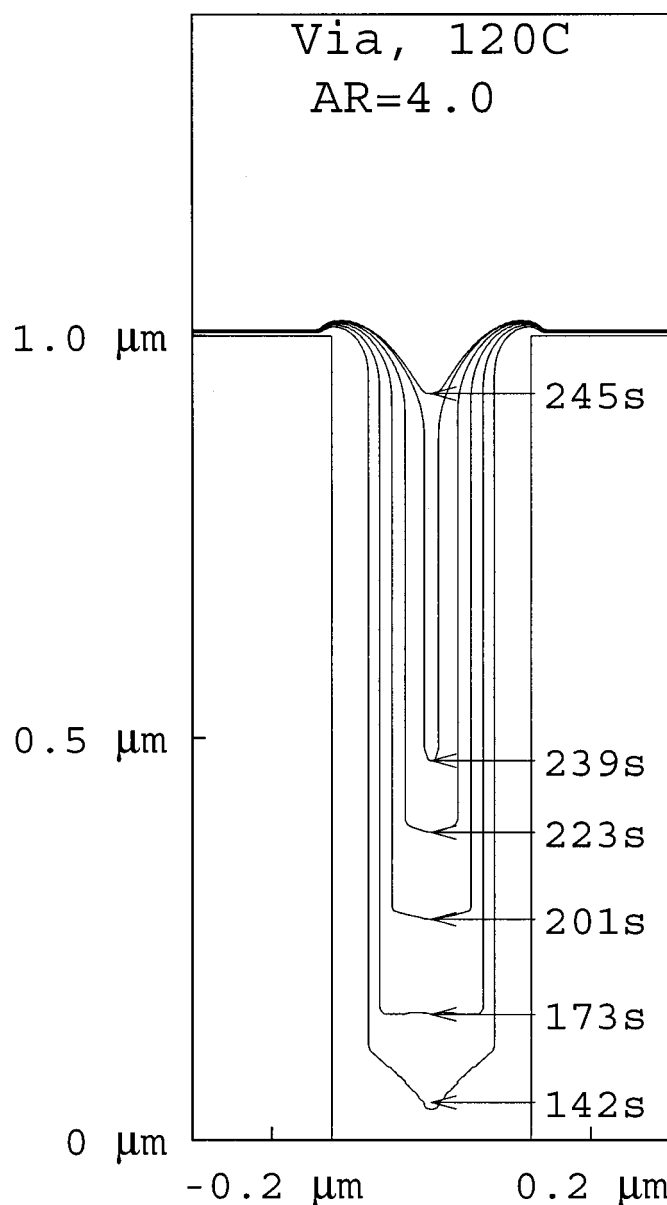
Figure 7. Predicted fill contours and times for deposition in a 1 μm high, 250 nm diam via for filling at 120°C and initial iodine coverage of 1.3×10^{-11} mol/cm^2 (corresponding to $\theta_o = 0.05$) for comparison to Fig. 4. The sidewalls are predicted to impinge between 239 and 245 s.

perature would enable filling of higher aspect ratio trenches by increasing the differential velocity $v(1,T)/v(\theta_o,T)$, though resulting in longer deposition times.

The filling simulations.—Iodine coverage on the free surface is presumed to be zero in the modeling, as intended by the soft plasma processing and manifest in the minimal deposition on those surfaces in the experiments (Fig. 4 and 5). Figure 7 shows predictions obtained using conditions that correspond to the via filling experiment in Fig. 4. Consistent with the experimental results, bottom-up deposition is evident for the aspect ratio 4 via at 120°C. However, sidewall impingement between 239 and 245 s, indicative of failure to fill, prevents its completion. Both the predicted bottom-up filling and the acceleration of the sidewalls are induced by the CEAC mechanism (*i.e.*, change of local catalyst coverage induced by changing area). It is unclear whether experiment and prediction
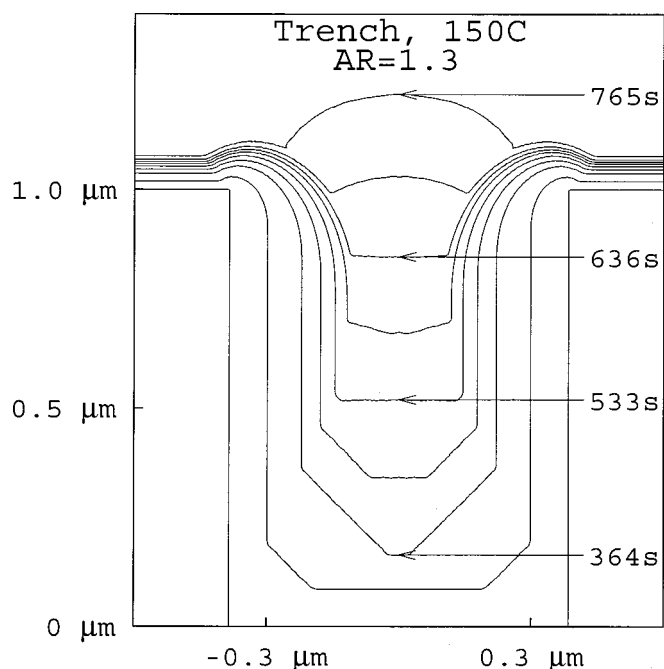
Figure 8. Predicted fill contours and times for deposition in a 1 μm high, 600 nm wide trench for filling at 150°C and initial iodine coverage of 1.3 × 10^{-11} mol/cm^2 (corresponding to $\theta_o = 0.05$) for comparison to Fig. 5.

match toward completion of filling; specifically, it is unclear if there is a void toward the top of the via (Fig. 4 at 300 s), as predicted by the simulation in Fig. 7.

Figure 8 shows predictions for the trench filling experiment in Fig. 5. Superconformal filling of the 1.3 aspect ratio trench is predicted for the 150°C deposition temperature, in agreement with the experimental result. The simulation captures the experimentally observed inception of superconformal filling at the bottom corners and the overfill bump. The filling time is not as well predicted. Figure 9 shows simulations of the trench filling experiments in Fig. 6; consistent with the experimental results, fill is predicted for 150°C and aspect ratio 3 while seam formation (*i.e.*, failure to fill) is predicted for 170°C and aspect ratio 3.5. Note that a void extending farther down the trench than the seam would be predicted by a code that included depletion[2] for the feature filled at 170°C.

Discussion

Though transport-limited deposition has not been modeled here, its impact should generally be considered. Indeed, operation near the crossover between interface kinetic and transport-limited deposition is evident; a ≈50% drop of the copper precursor concentration near the surface is suggested by the 0.4 nm/s deposition rate on the planar substrates (150°C, 30 s iodine exposure) that is half the estimated transport-limited deposition rate of 0.6 to 1 nm/s (based on Fig. 2c). Just doubling the surface area (100% increase) would lead to increased precursor consumption that, for the 150°C temperature and precursor operating conditions used here, would necessarily lead to transport-limited deposition. Note that 1 μm deep trenches spaced 0.5 μm (*e.g.*, Fig. 6) result in a 400% increase of surface area relative to that for the planar surface.

In spite of the simplifications of the particular CEAC-based model used, including neglect of transport-limited deposition, the model accurately predicted when trenches filled or failed to fill superconformally. The model also predicted the observed inception of superconformal filling at the bottom corners of the trenches and the development of a bump over the filled trenches. This was accomplished with no fitting parameters, as all kinetic parameters for the

(a)

(b)
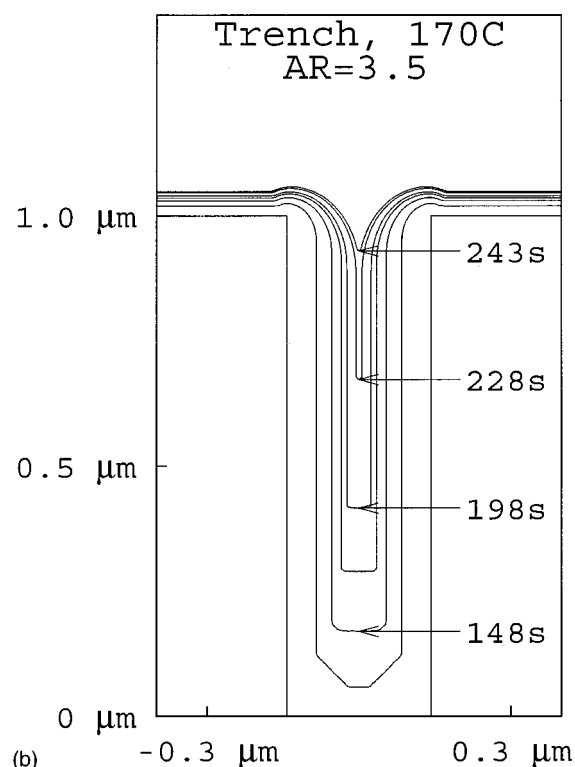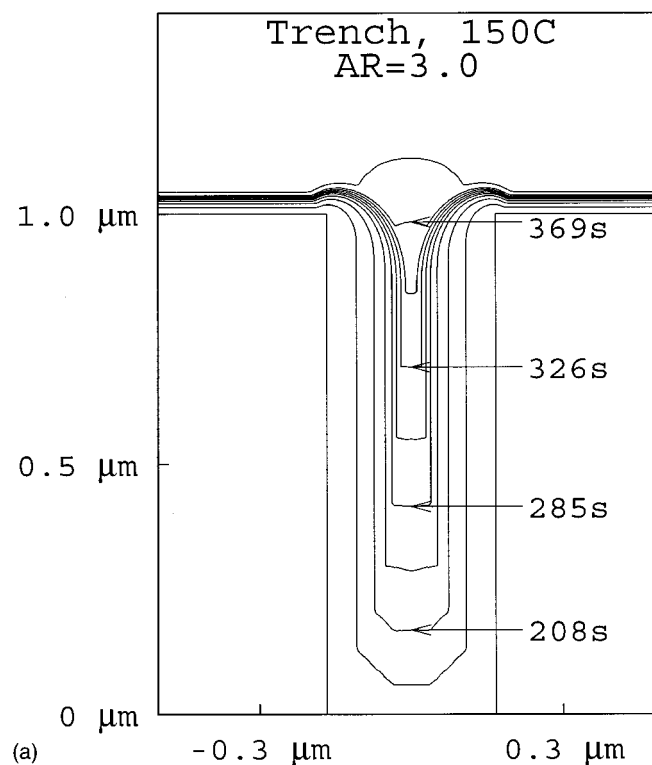
Figure 9. Predicted fill contours and times for (a) deposition in a trench of aspect ratio 3 filling at 150°C and (b) deposition in a trench of aspect ratio 3.5 filling at 170°C. The first case fills superconformally. In the second case the sidewalls impinge at ≈235 s, resulting in seam formation in the upper portion of the trench. Both simulations are for 1 μm high trenches with iodine coverage of 1.3 × 10^{-11} mol/cm^2 (corresponding to $\theta_o = 0.05$) for comparison to Fig. 6.

modeling were obtained from independent studies of deposition on planar substrates.

Two issues related to accuracy of predictions should be addressed in future efforts. First, predictions of the CEAC model can only be as accurate as the input kinetics; a study of the full $v(\theta, T)$ relationship should be experimentally obtained over the full $\theta:[0,1]$ range for temperatures of interest. Second, as noted above, transport of the copper precursor through the boundary layer and within the feature must be evaluated simultaneously with the interface kinetics already considered here. This has already been done for CEAC-based models of electrodeposition.[2] Such a result will necessarily be specific to the geometry of the particular system. However, detailed information on the impact of ambient vapor pressure of copper precursor on deposition rate, as well as measurements of boundary layer thickness and precursor diffusion coefficient would benefit all modeling efforts. Both inaccurate interface kinetics and neglect of transport in the modeling, including over the entire substrate wafer, likely did affect the accuracy of the predictions obtained here.

Conclusions

This work has used the CEAC mechanism to quantify superconformal filling of fine features by iodine-catalyzed CVD of copper in a manner similar to that recently done for copper and silver electrodeposition. The CEAC-based model accounts for changing coverage of adsorbed deposition rate-accelerating catalyst arising from changing surface area. Kinetics for simulations were obtained from studies of deposition on planar substrates. Taken as a whole, the results are consistent with the CEAC mechanism being the origin of superconformal filling during iodine catalyzed CVD.

An important implication of the agreement between the experimental and modeling results is that superconformal filling during CVD processes need not be limited to copper (a conclusion also reached by other authors.[11]) Superconformal feature filling by electrodeposition has already been accomplished with both copper and silver.[1-4,6] The only conditions that must be met for superconformal filling to occur with other metal systems are: (1) the rate-limiting step in the CVD process occurs on the deposit surface (rather than in the vapor) and (2) the kinetics of that rate-limiting step can be accelerated through interaction with an adsorbed catalytic surfactant that is not consumed (or is consumed very slowly) in the deposition process. For the case of copper CVD from precursor molecules that include hfac ligand(s), it has been suggested that the rate-limiting step is the removal and/or desorption of the hfac ligand, possibly through a disproportionation process that converts two adsorbed Cu-(hfac) to one $Cu(hfac)_2$, that volatilizes, and a Cu that remains as the metal deposit.[17,18] Based on the results presented here, the presence of the adsorbed iodine accelerates this process. This is supported by experimental results for iodine-catalyzed copper CVD using a different (hfac)Cu-based precursor, specifically (hfac)Cu(3,3-dimethyl-1-butene).[19] Note that, while the addition of H_2 can accelerate copper deposition through formation and volatilization of H(hfac) on the deposit surface, it cannot result in superconformal filling because the adsorbed "catalyst" is completely consumed in the process.[17]

Several forward looking speculative ideas are now put forth. First, the increased deposition rate of tantalum oxide during codeposition with relatively small amounts of palladium precursor[20] raises hopes for superconformal tantalum oxide deposition by CVD. Superconformal filling applications will require that the Pd catalyst segregates to the surface during growth; something that has not yet been ascertained. Second, the existence of molecules for Ag CVD that include the hfac ligand; Ag being a noble metal like Cu, suggests such precursors as a starting point for superconformal Ag CVD. Third, for Al CVD from trimethlamine alane $(CH_3)_3N)AlH_3$, cleavage of the Al-N bond connecting the Al and the ligand of the adsorbed molecule is the rate-limiting step.[21] A catalyst for this reaction that adsorbs on the surface without being consumed, desorbed, or buried would be expected to result in superconformal Al deposition. Finally, though no suggestion is made for approaching superconformal CVD of tungsten, the use of tungsten for microelectromechanical systems and as the front end metallization for transistor contacts in copper metallizations makes its consideration for future superconformal deposition studies worthwhile.

References

1. T. P. Moffat, D. Wheeler, W. H. Huber, and D. Josell, *Electrochem. Solid-State Lett.,* **4**, C26 (2001).
2. D. Josell, D. Wheeler, W. H. Huber, and T. P. Moffat, *Phys. Rev. Lett.,* **87**, 016102 (2001).
3. D. Josell, D. Wheeler, W. H. Huber, J. E. Bonevich, and T. P. Moffat, *J. Electrochem. Soc.,* **148**, C767 (2001).
4. T. P. Moffat, B. Baker, D. Wheeler, J. E. Bonevich, M. Edelstein, D. R. Kelly, L. Gan, G. R. Stafford, P. J. Chen, W. F. Egelhoff, and D. Josell, *J. Electrochem. Soc.,* **149**, C423 (2002).
5. D. Josell, D. Wheeler, and T. P. Moffat, *Electrochem. Solid-State Lett.,* **5**, C49 (2002).
6. T. P. Moffat, J. E. Bonevich, W. H. Huber, A. Stanishevsky, D. R. Kelly, G. R. Stafford, and D. Josell, *J. Electrochem. Soc.,* **147**, 4524 (2000).
7. E. S. Hwang and J. Lee, *Electrochem. Solid-State Lett.,* **3**, 138 (2000).
8. H. Park, W. Koh, S.-M. Choi, K.-C. Park, H.-K. Kang, J.-T. Moon, K. Shim, H. Lee, O. Kwon, and S. Kang, in *Proceedings of The IEEE 2001 International Technology Conference*, p. 12-14, June 4-6, 2001.
9. S. G. Pyo, W. S. Min, H. D. Kim, S. Kim, T. K. Lee, S. K. Park, and H. C. Sohn, in *Advanced Metallization Conference 2001*, MRS, p. 209 (2001).
10. D. Josell, D. Wheeler, and T. P. Moffat, *Electrochem. Solid-State Lett.,* **5**, C44 (2002).
11. K.-C. Shim, H.-B. Lee, O.-K. Kwon, H.-S. Park, W. Koh, and S.-W. Kang, *J. Electrochem. Soc.,* **149**, G109 (2002).
12. E. S. Hwang and J. Lee, *Chem. Mater.,* **12**, 2076 (2000).
13. P. H. Citrin, P. Eisenberger, and R. C. Hewitt, *Phys. Rev. Lett.,* **45**, 1948 (1980).
14. B. Di Cenzo, G. K. Wertheim, and D. N. E. Buchanan, *Surf. Sci.,* **121**, 411 (1982).
15. B. V. Andryushechkin, R. E. Baranovsky, K. N. Eltsov, and V. Y. Yurov, *Surf. Sci.,* **488**, L541 (2001).
16. S. G. Pyo, W. S. Min, and S. B. Kim, Unpublished work.
17. G. L. Griffin and A. W. Maverick, in *The Chemistry of Metal CVD*, T. Kodas and M. Hampden-Smith, Editors, p. 175, VCH Publishers, New York (1994).
18. M. J. Hampden-Smith and T. Kodas, in *The Chemistry of Metal CVD*, T. Kodas and M. Hampden-Smith, Editors, p. 239, VCH Publishers, New York (1994).
19. W. H. Lee, B. S. Seo, I. J. Byun, Y. G. Ko, J. Y. Kim, J. G. Lee, and E. G. Lee, *J. Korean Phys. Soc.,* **40**, 107 (2002).
20. K. D. Pollard and R. J. Puddephatt, *Chem. Mater.,* **11**, 1069 (1999).
21. M. G. Simmonds and W. L. Gladfelter, in *The Chemistry of Metal CVD*, T. Kodas and M. Hampden-Smith, Editors, p. 45, VCH Publishers, New York (1994).